J Nanopart Res (2015)17:198
DOI 10.1007/s11051-015-3009-2

RESEARCH PAPER

Improved DNA condensation, stability, and transfection with alkyl sulfonyl-functionalized PAMAM G2

Azahara Rata-Aguilar · Julia Maldonado-Valderrama · Ana Belén Jódar-Reyes · Juan Luis Ortega-Vinuesa · Francisco Santoyo-Gonzalez · Antonio Martín-Rodríguez

Received: 28 January 2015 / Accepted: 16 April 2015

Abstract In this work, we have used a second-generation PAMAM grafted with octadecyl sulfonyl chains to condense plasmid DNA. The influence of this modification at different levels was investigated by comparison with original PAMAM G2. The condensation process and temporal stability of the complexes was studied with DLS, finding that the aliphatic chains influence DNA compaction via hydrophobic forces and markedly improve the formation and temporal stability of a single populated system with a hydrodynamic diameter below 100 nm. Interaction with a cell membrane model was also evaluated with a pendant drop tensiometer, resulting in further incorporation of the C18-PAMAM dendriplexes onto the interface. The improvement observed in transfection with our C18 grafted PAMAM is ascribed to the size, stability, and interfacial behavior of the complexes, which in turn are consequence of the DNA condensation process and the interactions involved.

A. Rata-Aguilar (✉) · J. Maldonado-Valderrama · A. B. Jódar-Reyes · J. L. Ortega-Vinuesa · A. Martín-Rodríguez
Biocolloid and Fluid Physics Group, Department of Applied Physics, University of Granada, Fuentenueva s/n, 18071 Granada, Spain
e-mail: azahara@ugr.es

F. Santoyo-Gonzalez
Organic Chemistry Department, Institute of Biotechnology, University of Granada, 18071 Granada, Spain

Keywords Gene delivery · Dendriplex · PAMAM · Hydrophobic interactions · Interfacial rheology · Transfection

Introduction

Dendrimers are polymers with unique properties, highlighting the perfectly defined and monodisperse structure (based on stepwise synthesis) and multiple terminal groups. These features make dendrimers useful for biomedical applications (Mintzer and Grinstaff 2011) as antimicrobial and antiviral drug, in tissue engineering, drug delivery, transfection, and others (Dufes et al. 2005; Kaminskas et al. 2014; McCarthy et al. 2013; Peng et al. 2013; Somani et al. 2014).

When it comes to gene delivery, polyamidoamines (PAMAM) are one of the most widespread dendrimers. PAMAM bears surface amino groups which facilitates the electrostatic interaction with the negatively charged DNA. Moreover, the buffering capacity of the internal amino groups is believed to facilitate endosomal escape due to the proton sponge effect. Haensler and Szoka (1993) published the first gene delivery study using PAMAM to form a dendrimer-DNA complex (dendriplex). Many papers have followed, reaffirming the potential suitability of PAMAM for gene delivery (Eichman et al. 2000; Shcharbin et al. 2013).

Published online: 28 April 2015

However, in spite of their promising features, 20 years later dendriplexes have not been translated into the clinic. It is still a challenge to predict the in vivo behavior of synthetic vectors and there is a need for optimization and rational design of polymeric therapeutics (Duncan and Vicent 2013). Characterization of dendriplexes at the physicochemical, in vitro and in vivo levels (Shcharbin et al. 2009, 2010, 2014) is essential to achieve the desirable outcome (Gimenez et al. 2012; Merkel and Kissel 2014).

In a previous paper, we carried out an extensive study upon synthesis and in vitro evaluation of alkyl vinyl sulfone derivatives of PAMAM G2 via aza-Michael addition and came out with some useful engineered dendrimers (Morales-Sanfrutos et al. 2011). The attachment of hydrophobic moieties to the original structure of PAMAM is not new and several modifications can be found in the literature. Aliphatic chains (Santos et al. 2010), steroids (Choi et al. 2006), hydrophobic aminoacids (Kono et al. 2005), or even organic fluorescent dyes (Yoo and Juliano 2000) all seem to agree on the improvement in transfection. In most cases, this fact is ascribed to a facilitated interaction with cell membranes, even though it seems unlikely for some of the moieties used.

Therefore, in the present paper, we will discuss the implications of aliphatic modification of PAMAM at different levels: (a) formation and stability of dendriplexes, (b) interaction with a cell membrane model, and (c) transfection efficiency. For that purpose, we have chosen from our previous work the 6c-G2(I) dendrimer, an octadecyl-modified C18-PAMAM G2 (structure shown in Fig. 1). The significant improvements in DNA condensation and transfection achieved by incorporation of a C18 alkyl chain to PAMAM G2 are described.

Materials and methods

Synthesis of modified PAMAM G2 dendrimer

The detailed synthesis procedure is explained in (Morales-Sanfrutos et al. 2011). Briefly, the original bromide functionality of 1-bromooctadecane was replaced by the vinyl sulfonyl group. The obtained vinyl sulfone derivative (0.15 mM, tetrahydrofuran (THF) 15 ml) was added to a solution of PAMAM-G2 (0.3 mM, milliQ-water 15 mL). The mixture was magnetically stirred at room temperature for 1 day. Then the solvent (THF) was evaporated under reduced pressure and the water was freeze-dried. The product was used directly. Generation 2 PAMAM dendrimer (PAMAM-G2) was purchased from Aldrich. Commercially available reagents and solvents were used as purchased without further purification.

Formation of dendrimer/DNA complexes

The plasmid DNA used in this work corresponds to the GFP-encoding plasmid pEGFP-C1 (Clontech Laboratories, Inc., Palo, Alto, CA). It has 4.7 kbp (kilobase pairs) and it was kindly provided by Dr. Márquez, University of Málaga (Spain). Plasmid DNA was amplified and purified using the GenElute Gigaprep Kit (Sigma-Aldrich (Milwaukee, USA)) following manufacturer's instructions. DNA working solution at 20 μg/mL was prepared in HEPES 5 mM pH 7.4. Dendrimer stock solutions were prepared in a mixture of DMSO: water (1:2) at a concentration up to 20 mg/mL. Working dilutions of each dendrimer were prepared prior to each use in HEPES buffer 5 mM at pH 7.4. The DNA solution was then added to an equal volume of the dendrimer solution (containing the desired concentration) and immediately mixed by thorough pipetting. The complexes were allowed to self-assemble at room temperature for 30 min and the final DNA concentration was 0.024 nM (Concentration of phosphate groups, [P]). Unless stated otherwise, all chemicals and reagents were purchased from Sigma-Aldrich (Milwaukee, USA). The ratio between DNA and dendrimer was expressed as $Z = \text{N/P}$, the ratio between protonable nitrogen residues of the dendrimer and DNA phosphate groups.

Size measurement

The average size of the dendriplexes was determined by dynamic light scattering (DLS) using a Zetasizer NanoZeta ZS device (Malvern Instruments Ltd, U.K.) working at 25 °C with a He–Ne laser beam ($\lambda_0 = 633$ nm) and using a scattering angle of 173°. For data analysis, the viscosity (0.8905 mPa/s) and refractive index (1.333) of pure water at 25 °C were used. Results are given as mean values of three runs of 60-s duration each. The intensity of scattered light was also recorded as kilocounts per second (kcps). All measurements were carried out in duplicates at 25 °C.

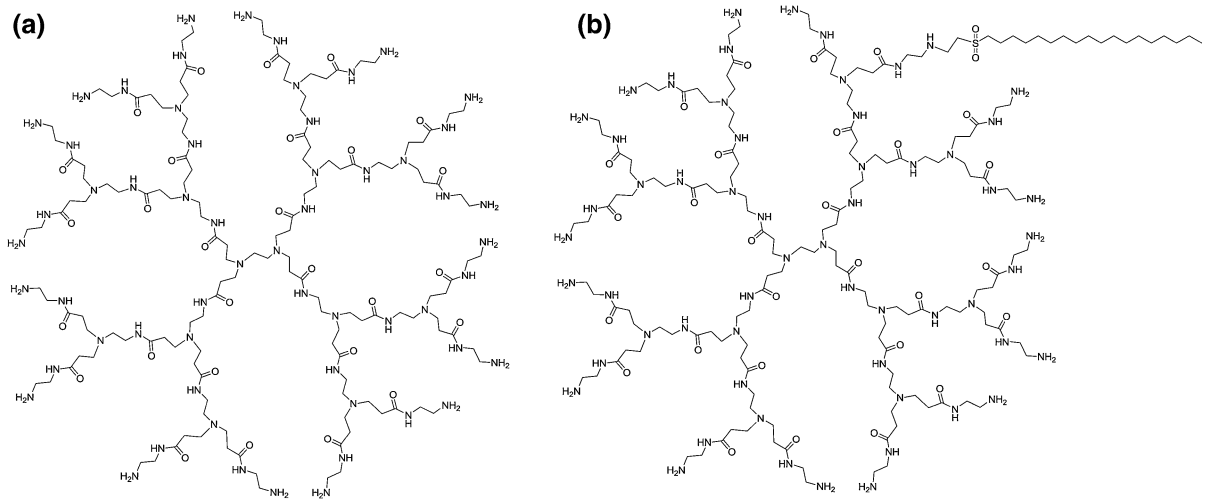

Fig. 1 Chemical structures of **a** PAMAM G2 and **b** PAMAM G2 modified with a C18 alkyl sulfonyl chain (1:0.5) via aza-Michael addition (C18-PAMAM)

Electrophoretic mobility

The electrophoretic mobility of the dendriplexes, which is related to the effective surface charge of the particles, was measured by the technique of laser Doppler electrophoresis with a Zetasizer NanoZeta ZS (Malvern Instruments Ltd, Worcestershire, U.K.) using folded capillary cells. All measurements were carried out in duplicates at 25 °C.

Gel retardation

Formation of dendriplexes was also determined by gel retardation using the electrophoretic mobility shift assay (EMSA). After complex formation at different N/P ratios, the samples were electrophoresed on a 1 % (w/v) agarose gel at 100 V. After 40 minutes the gel was stained in a 3X GelRed® solution (Labnet biotécnica, Madrid), analyzed on a UV illuminator, and photographed.

Surface tension and interfacial rheology

The surface characterization of the mixed system has been made in the OCTOPUS. This a Pendant Drop Surface Film Balance equipped with a subphase multi-exchange device fully designed and assembled at the University of Granada (patent submitted P201001588) and described in detail in (Maldonado-Valderrama et al. 2013). The detection and calculation of surface area and surface tension are done with the DINATEN® software, based on axisymmetric drop shape analysis (ADSA).

An HEPES solution droplet is formed first at the tip of the double coaxial capillary. By deposition with a microsyringe, a fixed amount of DPPC is spread onto the drop surface to provide a surface pressure of 20 mN/m. After evaporation of the solvent and equilibration of the surface pressure, the buffer subphase is exchanged by simultaneously injecting the new solution and extracting the bulk subphase (Maldonado-Valderrama et al. 2014; Wege et al. 2002). After complete exchange of the subphase, we monitor the surface pressure at constant surface area for 20 min. Finally, we measured the dilatational rheology of this surface layer by imposing cycles of 10 oscillations at different frequencies to the drop. The dilatational modulus (E) of the interfacial layer is calculated by the image analysis program CONTACTO®. The reproducibility of the experiments was tested by performing at least three replicate measurements. The surface tension of the clean surface was measured before every experiment, in order to confirm the absence of surface-active contaminants, yielding values of 72.5 ± 0.5 mN m^{-1} at 20 °C.

Cell culture

HeLa cells were grown in DMEM (Sigma-Aldrich, Milwaukee, USA) supplemented with 1 % non-

essential amino acids and 10 % fetal bovine serum (FBS), at 37 °C and 5 % CO2.

Transfection efficiency

HeLa cells were seeded into 24-well plates at a density of 100,000 cells/well. After 24 h, culture medium was replaced with 400 μL fresh serum-free DMEM. Dendriplexes at corresponding N/P ratios in 100 μL Hepes buffer (5 mM, pH 7.4), containing 0.5 μg pDNA were added to each well and incubated at 37 °C for 40 min. Growth medium was replaced with supplemented DMEM (10 % FBS, 1 % non-essential aminoacids) and cells were incubated for further 24 h. Subsequently, cells were washed twice with 500 μL PBS, detached with trypsin/EDTA and taken up in PBS. GFP expression was evaluated by flow cytometry (BECTON–DICKINSON FACSCanto II). Cells transfected with branched PEI, 25 kDa at a N/P ratio of 6 were used as positive control.

In vitro toxicity

HeLa cells were seeded into 96-well plates at a density of 10,000 cells/well. After 24 h, culture medium was replaced with 80 μL fresh DMEM. pDNA dendriplexes at corresponding molar ratios in 20 μL Hepes buffer (5 mM, pH 7.4), containing 100 ng pDNA were added to each well and incubated at 37 °C for 40 min. Growth medium was replaced with supplemented DMEM (10 % FBS, 1 % non-essential aminoacids) and cells were cultured for an additional 24 h. Culture media were replaced with 100 μl of fresh media and then 50 μl of MTT (3-(4,5-dimethylthiazol-2-yl)2,5- diphenyltetrazolium bromide) reagent (5 mg/ml in PBS) was added to each well. Following a 4-h incubation at 37 °C, medium was replaced with 100 μl/well of solvent (50 % DMSO, 50 % isopropanol). Absorbance at 570 nm was read in a Nanoquant Infinite M200 Pro (Tecan) analyzer. Untreated cells were used as positive control (100 % viable).

Results and discussion

DNA condensation

In a first approach, we studied the ability of the of PAMAM and C18-PAMAM G2 dendrimers (structures shown in Fig. 1) to condense DNA. The hydrodynamic diameter and surface charge at different Z were evaluated and the results are shown in Fig. 2. It is important to note that the size obtained by DLS is the diameter that an equivalent spherical particle would have in solution.

When low quantities of dendrimer are used, large aggregates appear in solution. Close to the neutralization point, aggregation of non-charged complexes occurs. If we increase Z, we finally obtain particles of lower hydrodynamic diameter. The first difference we can observe is related to the average diameter of the particles. Much lower values are found when C18-PAMAM is used. The hydrophobic chain bound to C18-PAMAM contributes to better condensation of DNA, obtaining particles with an approximate average diameter of 80 nm. On the other hand, unmodified PAMAM yields bigger particles which become even bigger if we continue adding dendrimer.

In Fig. 2b, we can observe the electrophoretic mobility of the resulting complexes. Both curves are similar, as expected due to the low modification ratio, which barely changes the overall charge of the PAMAM dendrimers. The surface charge of the complexes remains constant and positive over a $Z = 5$.

The intensity- and volume-weighted size distributions of our complexes obtained from the DLS data as a function of Z for both dendrimers are shown in Fig. 3. The evolution of the system upon progressive addition of dendrimer can be followed from top to the bottom. At the point of charge neutrality, we find large aggregates of around 1 μm for both dendrimers. We will focus first on the solid lines in Fig. 3, corresponding to dendriplexes of C18-PAMAM. In the region $Z = 5$–12, it is evident the coexistence of two different populations (Dias et al. 2005). On the one hand, we find a broad peak which might correspond to a coil or extended conformation, with fluctuations as indicated by the width of the peak. On the other hand, we can see a narrower peak of more compact small particles that becomes predominant when increasing the dendrimer concentration. (Note that the x-axis scale is logarithmic).

If we observe now the dotted lines in Fig. 3, that is, dendriplexes of PAMAM, some differences are found. We can also see coexistence, but both peaks are displaced into higher values. Besides, the proportion between the two populations remains basically constant even at high Z.

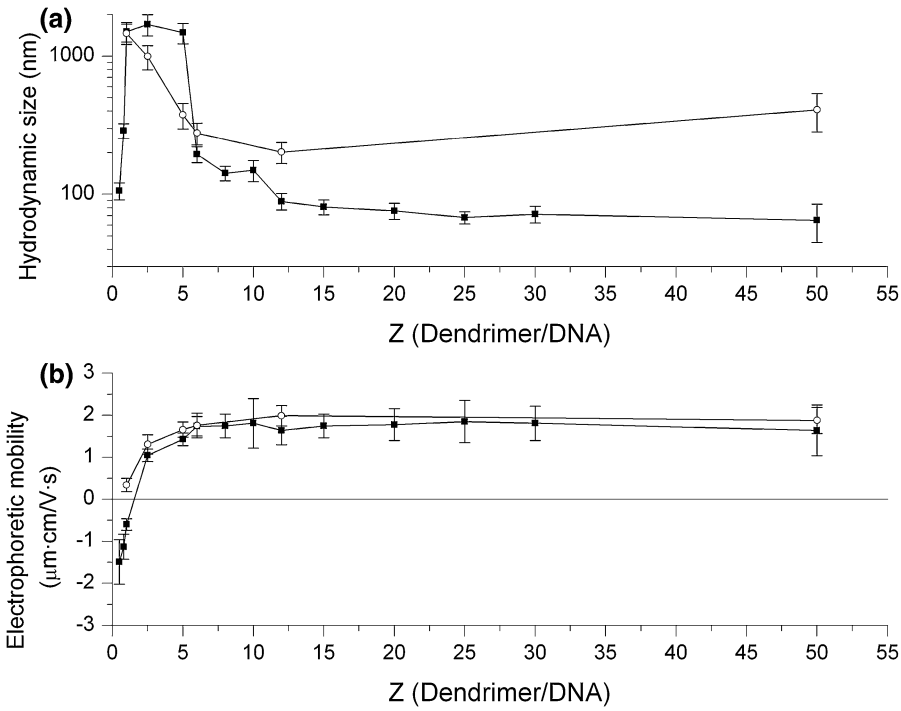

Fig. 2 **a** Average hydrodynamic diameter and **b** average electrophoretic mobility, at various *Z* of PAMAM (*open circle*) and C18-PAMAM (*filled square*) dendriplexes

PAMAM dendrimers present primary amino groups on their surfaces, so they are positively charged at pH 7.4. Due to the negative charge of DNA, there will be electrostatic attraction between them, yielding to interpolyelectrolyte complexes (IPEC) as observed in EMSA studies (Fig. 4), where all DNA is retained above N/P ratios of 1. In order to be used for gene delivery, the dendrimers should condense DNA into small particles that are able to pass more easily through the biological barriers. It is though not enough to obtain an IPEC, but the polymers must blend into more compact particles, presumably with a toroidal shape in the case of second-generation PAMAM (Qamhieh et al. 2014). According to our results, for both modified and unmodified PAMAM, IPEC are formed with DNA. But only when the alkyl C18 chains are present, small compact and predominant particles are obtained.

Temporal stability of the complexes

After analyzing particle size distributions, we decided to focus on focus on $Z = 12$, which is the lowest proportion we found with acceptable homogeneity of C18-PAMAM samples (percentage of intensity corresponding to compact particles over 80 %). PAMAM and C18-PAMAM dendriplexes at $Z = 12$ were allowed to evolve with time while we measured their diameter every 5 min. Figure 4a, b show the hydrodynamic diameter of the dendriplexes taken from the position of the main and secondary peaks of the intensity distribution given by the DLS device. (Note: Only the main and secondary peaks corresponding to intensity percentages higher than 20 % are considered for clarity.)

As observed in Fig. 5a, C18-PAMAM dendriplexes have a hydrodynamic diameter of 60 nm and they are stable for at least 18 h in formulation buffer. However, some aggregates of approximately 300–400 nm start to appear after 10 h.

On the other hand, PAMAM dendriplexes, as seen in Fig. 5b, present two peaks from the beginning corresponding to extended complexes and compact particles. It is easy to follow the evolution of both populations, which remain constant up to 40 min. At this point, bigger particles become predominant in terms of intensity, and their size starts to increase progressively. Two hours later the device is not able to detect any of the smaller particles, either because of their disappearance or due to the impossibility of DLS to distinguish small (and scarce) particles when much bigger ones are present.

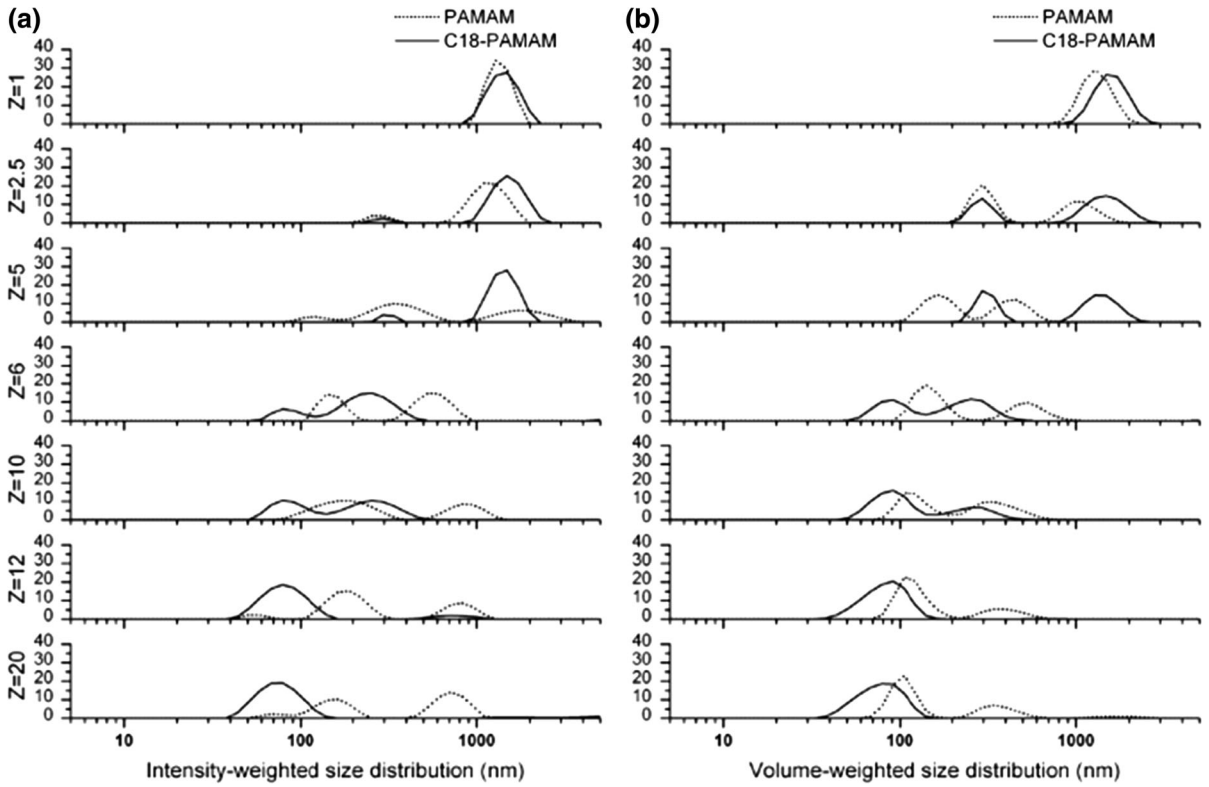

Fig. 3 **a** Intensity-weighted distribution functions and **b** volume-weighted distribution functions of PAMAM (*dotted line*) and C18-PAMAM (*solid line*) dendriplexes at various Z

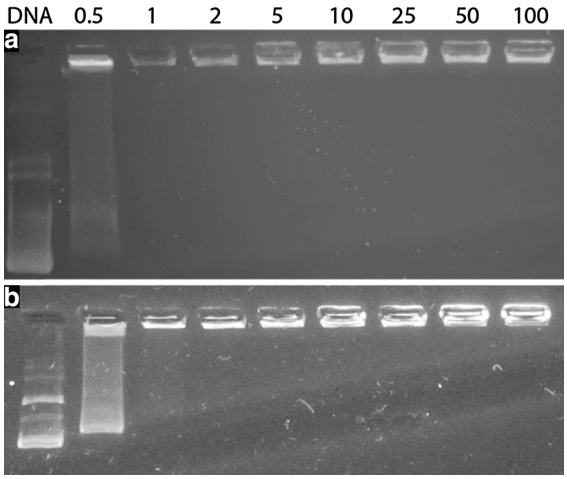

Fig. 4 Electrophoresis mobility shift assay of dendriplexes formed with **a** PAMAM and **b** C18-PAMAM at indicated N/P ratios

The increase in size might be caused by aggregation of the dendriplexes or decompaction of DNA. We have used static light scattering to solve which of these two situations occurs. Figure 6 gives information about the time evolution of scattered intensity. Aggregation will be distinguishable as an increase in the scattered light. On the contrary, if there is dissociation, the scattered light intensity will drop.

It is clear from Fig. 6 that the temporal behavior of both systems is different. In the case of PAMAM dendriplexes, there is no appreciable change in the intensity during the first 100 min (after 30 min of condensation, this is, 130 min from mixing). After that, a fast decrease is observed, indicating disassembly due to morphological changes experienced by low generation PAMAM dendriplexes, as explained elsewhere (Carnerup et al. 2009). From these results it is deduced that after mixing PAMAM G2 and DNA, an unstable state is reached and the system quickly evolves into a more stable configuration. But this instability can be avoided thanks to the added alkyl chains in our C18-PAMAM. Despite the evident process of progressive slow aggregation deduced by the slight slope of the scattered light intensity (Fig. 6),

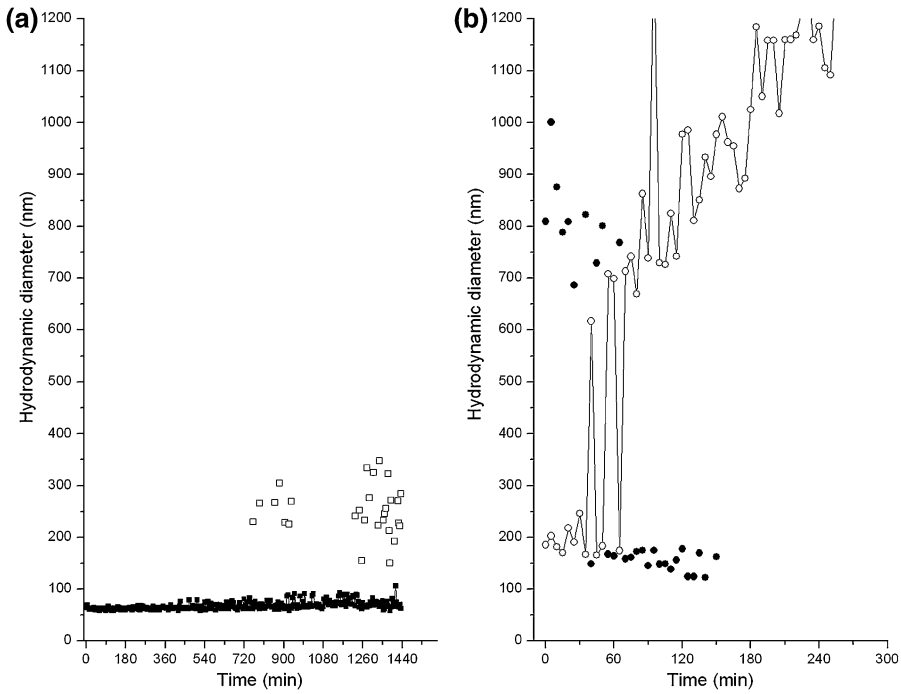

Fig. 5 Temporal evolution of the mean diameters of the various peaks from the intensity distribution functions given by DLS of **a** C18-PAMAM dendriplexes, main peak *filled square*, secondary peak *open square* and **b** PAMAM dendriplexes, main peak *open circle*, secondary peak *filled circle* at $Z = 12$

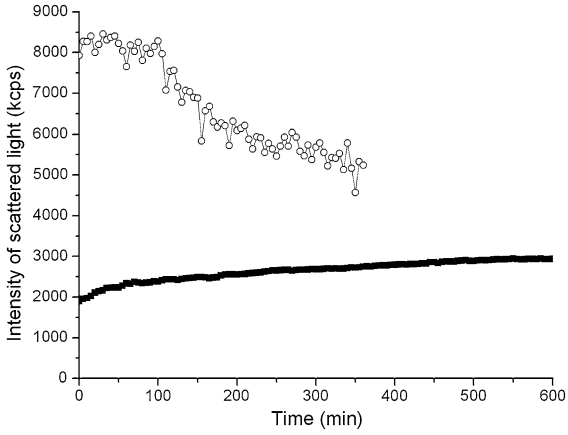

Fig. 6 Temporal evolution of the intensity of light scattered by C18-PAMAM (*filled square*) and PAMAM (*open circle*) dendriplexes at $Z = 12$

the 60 nm population of C18-PAMAM dendriplexes remains unchanged for at least 20 h (Fig. 5a). This is a huge improvement compared to original PAMAM.

Interaction with a cell membrane model at the water–air interface

Once demonstrated that the PAMAM-bearing alkyl chains with 18 carbon atoms improves the condensation of the DNA in the dendriplex due to hydrophobic forces, it is interesting to evaluate whether this modification also affects the interaction with a model cell membrane. We have evaluated both the adsorption kinetics of our dendriplexes onto a monolayer of zwitterionic lipid DPPC (dipalmitoylphosphatidylcholine) and the rheological properties of the mixed DPPC/dendriplex system. These experiments, which to our knowledge have not been performed before with dendriplexes, have been carried out in a pendant drop film balance implemented with subphase exchange so that the interaction can be analyzed in situ and with minimal disturbance of the surface (Maldonado-Valderrama et al. 2014b).

Figure 7a shows the time evolution of the surface pressure of a DPPC monolayer spread onto HEPES buffer following subphase exchange by dendriplex or HEPES solution at a surface pressure of 20 mN/m before exchange. Note that the data plotted in Fig. 7a start after the subphase exchange had been completed so that the starting surface pressure is already different from 20 mN/m for the dendriplexes curves. A reference curve where we exchanged the drop subphase by the same buffer solution has been included in the figure for comparison. In this curve, the surface pressure remains constant at 20 mN/m. Exchange by

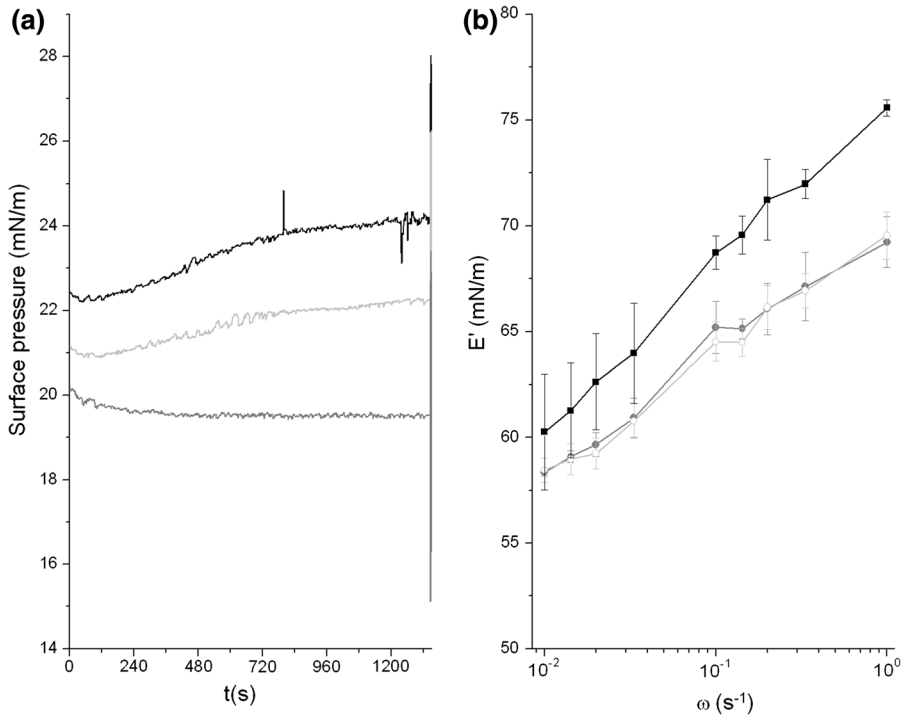

Fig. 7 **a** Adsorption kinetics onto a DPPC monolayer at $\pi = 20$ mN/m following subphase exchange with C18-PAMAM dendriplexes (*black*), with PAMAM dendriplexes (*light gray*), and with HEPES buffer (*gray*). **b** Dilatational surface elasticity moduli as a function of frequency measured at the end of curves plotted in (**a**). Subphase exchange of DPPC monolayer with C18-PAMAM dendriplexes (*black*), with PAMAM dendriplexes (*light gray*), and with HEPES buffer (*gray*)

PAMAM dendriplexes results in an increase in the surface pressure which is doubled in the case of C18-PAMAM complexes. The increase takes place during the exchange, as indicated by the different starting points of the curves, and it continues with time. The adsorption kinetics shows in both cases a small lag time after the exchange followed by a rapid increase of surface pressure reaching a steady state in 15 min. The small lag time recorded might indicate that the dendriplex sticks itself under the DPPC monolayer prior to penetrating into the surface layer(Pavinatto et al. 2007). DPPC is a zwitterionic lipid that bears a positive charge from the choline group and a negative charge from the phosphate. At the air–water interface, the polar heads of the phospholipids are oriented into the bulk so that the dendriplexes can interact electrostatically with the phosphate group (Berenyi et al. 2014). The increment of surface pressure shown in Fig. 6a clearly indicates that both PAMAM and C18-PAMAM dendriplexes are attracted onto the surface layer and penetrate into the phospholipid chains but the effect is more noticeable when the alkyl chain is present.

Penetration of the dendriplexes into the lipid monolayer could result in alterations of the lateral packing in the monolayer (Luque-Caballero et al. 2014). In order to investigate this in more detail, we measured the surface dilatational moduli of the adsorbed dendriplexes onto the DPPC monolayer. This magnitude reflects inter- and intramolecular interactions taking place at the surface and is sensitive to molecular orientations and conformational transitions at the surface (Maldonado-Valderrama et al. 2005). We measured the surface dilatational modulus at different frequencies of perturbation imposed to the oscillating drop. In all cases, the viscous component of the dilatational modulus was very small and the systems appear predominantly elastic. Hence, Fig. 7b shows the elastic component of the surface dilatational modulus (E') of DPPC, DPPC/dendriplex, and DPPC/C18-PAMAM dendriplex. The oscillations were done at the end of each dynamic curve shown in Fig. 6a.

Interestingly, Fig. 7b shows that only the presence of the C18-PAMAM complexes significantly affects the dilatational elasticity of the surface layer. This suggests that the hydrophobic modification of C18-PAMAM not only implies a further penetration into the DPPC monolayer but also affects the packing state of the monolayer in contrast with PAMAM dendriplexes. According to Fig. 3, PAMAM dendriplexes present an extended conformation (flexible), while C18-PAMAM condenses DNA into small particles (rigid). The increased stiffness observed with C18-PAMAM can be attributed to the presence of those rigid complexes at the surface. Also, the presence of the alkyl chains at the surface could promote molecular binding at the surface, hence resulting in a stiffer molecular assembly.

Figure 6b also shows that the dilatational elastic modulus increases with the oscillation frequency in all three curves as expected in the linear regime (Lopez-Montero et al. 2012). However, this increase is more noticeable (higher slope) for the DPPC/C18-PAMAM dendriplex. Thus, the higher the frequency the more visible the differences are between the two dendrimers. According to Lopez-Montero et al. (2012), this behavior could be ascribed to the formation of lipid domains induced by the C18-PAMAM dendriplexes meaning that the interaction occurs locally at the surface in domains. Accordingly, despite the minor surface activity of the dendriplexes, C18-PAMAM dendriplexes seem to promote a local distortion of the phospholipid tails.

We have looked into two magnitudes of the mixed lipid/dendriplex. On the one hand, the dynamic adsorption curves in Fig. 6a demonstrate that C18-PAMAM dendriplexes have stronger affinity for phospholipids at the air–water interface than PAMAM complexes. On the other hand, only C18-PAMAM dendriplexes affect the rheological properties of the monolayer. Hence, at a low surface coverage of DPPC ($\approx$20 mN/m), PAMAM dendriplexes penetrate into the DPPC monolayer interacting with the phospholipid molecules via electrostatic interactions. This mechanism barely affects the flexibility of the monolayer as measured by the dilatational elastic modulus. Conversely, C18-PAMAM dendriplexes penetrate into the DPPC monolayer interacting with the phospholipid molecules by a combined mechanism including electrostatic and hydrophobic interactions. The mechanism of DNA compaction of C18-PAMAM provides a stiffer system and the alkyl chain seems to induce lipid domains which could be significant for cellular uptake (Conner and Schmid 2003; Raykar et al. 1988).

Transfection efficiency and toxicity

The ultimate goal of our dendriplexes is to deliver efficiently plasmid DNA into cells. We used both systems at different Z to transfect HeLa cells with the GFP (Green Fluorescent Protein)-encoding plasmid pEGFP. Figure 8 shows the percentage of complete cells that expressed green fluorescent protein after transfection with our dendriplexes and the viability of treated cells.

When Z is increased, so is the transfection efficiency of both systems. Between $Z = 1$ and $Z = 5$, the increase in the positive charge of the complexes (Fig. 2) favors the interaction with the negatively charged cell surfaces, which is a requirement for unspecific cellular uptake. However, if we focus on the C18-PAMAM, we observe an augment in the percentage of transfected cells even when the charge of the complexes was constant; this is, from $Z = 5$ to $Z = 20$. This can be ascribed to the size distribution explained above (Fig. 3). When increasing Z, one small population was predominant, which is probably more efficient in delivering the plasmid (Bielinska et al. 1999).

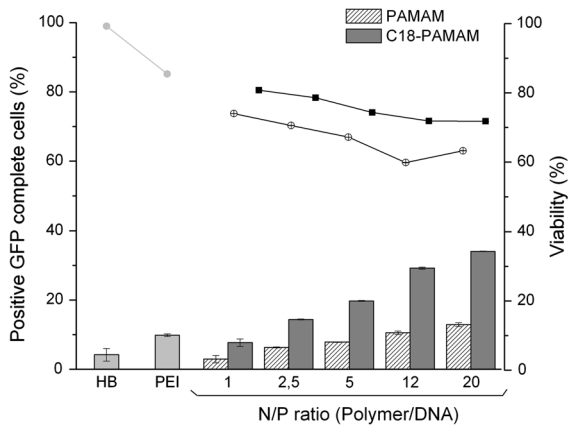

Fig. 8 Transfection efficiency (*bars*) and relative viability (*circles*). HeLa cells were transfected with PAMAM or modified PAMAM dendriplexes at indicated Z. Hepes buffer was used as negative control and PEI polyplexes at $Z = 6$ were considered positive control (*light gray*). PAMAM (Patterned bars, *open circle*), C18- PAMAM (*gray bars*, *filled square*)

If we compare now both systems, it is clear that the transfection efficiency of the C18-PAMAM dendriplexes is considerably enhanced. At the optimized $Z = 12$, a three-fold increase in transfection was observed when the hydrophobic chain was present. The incorporation of this alkyl chain influences the hydrophobicity, size, and stability of the complexes, which contribute to their interaction with cells, as seen in the cell membrane model, resulting in this case in enhanced GFP expression.

Cell viability is also shown in Fig. 8. PAMAM dendriplexes are slightly more toxic than their modified C18-PAMAM counterparts. It is known that the cytotoxic effects of polycations are related to their interaction with the negatively charged cell membrane which leads to destabilization and even activation of intracellular signaling pathways (Fischer et al. 2003). When the polycation is bound to DNA, the toxicity is reduced if compared to the polycation itself. In our case, unmodified PAMAM G2 was not efficient in condensing DNA, and disassembly was found in a short time. This means that the concentration of free dendrimer is higher and explains the higher toxicity.

Conclusions

An alkyl sulfonyl-modified PAMAM G2 was investigated as gene vector and compared to unmodified PAMAM G2. The dendrimers were used to condense plasmid DNA and both modified and unmodified PAMAM formed IPEC with DNA. Interestingly, incorporation of the C18 aliphatic chain helps to the condensation process via hydrophobic interactions resulting in a single population of small and compact complexes above $Z = 12$. This is in contrast with the multiple coexistent conformations found for the entire range of Z studied with PAMAM.

The temporal stability of the dendriplexes was also influenced by the condensation process and consequently by the added alkyl chains. Complexes formed with C18-PAMAM were ten-fold more stable in solution than the original PAMAM dendriplexes, which disassembled in few hours.

The interaction of our dendriplexes with a model membrane was addressed by pendant drop tensiometry obtaining an augmented incorporation of C18-PAMAM complexes into a lipid layer. Moreover, the experimental results evidence that, at low surface coverage, the dilatational elasticity of the lipid monolayer is not affected by the presence of PAMAM dendriplexes, whereas the C18-PAMAM dendriplexes increase the rigidity of the monolayer. The possible induction of lipid domains suggested by the interfacial rheology studies might have an effect on the internalization and should be further studied.

At the optimized $Z = 12$, a three-fold increase in transfection was observed when the hydrophobic chain was present. The incorporation of the octadecyl chains strongly influences the DNA condensation process modulating the size and stability of the complexes and their interaction with a model membrane, which results in better biological performance in vitro.

Acknowledgments The authors wish to express their appreciation for the financial support Granted by the following research projects: MAT2010-20370 (MICINN, Spain), MAT 2013-43922-R, P10-CTS-6270 (Junta de Andalucía, Spain), and CTQ 2011-29299-C02-01. Azahara Rata-Aguilar thanks the Government of Spain (MECD) and the University of Granada for her FPU fellowship. Alicia Megía-Fernández and Julia Morales-Sanfrutos are greatly acknowledged for their synthesis work (Morales-Sanfrutos et al. 2011).

References

Berenyi S, Mihaly J, Wacha A, Toke O, Bota A (2014) A mechanistic view of lipid membrane disrupting effect of PAMAM dendrimers. Colloids Surf B 118:164–171. doi:10.1016/j.colsurfb.2014.03.048

Bielinska AU, Chen CL, Johnson J, Baker JR (1999) DNA complexing with polyamidoamine dendrimers: implications for transfection. Bioconjugate Chem 10:843–850. doi:10.1021/Bc990036k

Carnerup AM, Ainalem ML, Alfredsson V, Nylander T (2009) Watching DNA condensation induced by poly(amido amine) dendrimers with time-resolved cryo-TEM. Langmuir 25:12466–12470. doi:10.1021/La903068v

Choi JS, Ko KS, Park JS, Kim YH, Kim SW, Lee M (2006) Dexamethasone conjugated poly(amidoamine) dendrimer as a gene carrier for efficient nuclear translocation. Int J Pharm 320:171–178. doi:10.1016/j.ijpharm.2006.05.002

Conner SD, Schmid SL (2003) Regulated portals of entry into the cell. Nature 422:37–44. doi:10.1038/Nature01451

Dias RS, Innerlohinger J, Glatter O, Miguel MG, Lindman B (2005) Coil-globule transition of DNA molecules induced by cationic surfactants: a dynamic light scattering study. J Phys Chem B 109:10458–10463. doi:10.1021/jp0444464

Dufes C, Uchegbu I, Schatzlein A (2005) Dendrimers in gene delivery. Adv Drug Deliv Rev 57:2177–2202. doi:10.1016/j.addr.2005.09.017

Duncan R, Vicent MJ (2013) Polymer therapeutics-prospects for 21st century: the end of the beginning. Adv Drug Deliv Rev 65:60–70. doi:10.1016/j.addr.2012.08.012

Eichman J, Bielinska A, Kukowska-Latallo J, Baker J (2000) The use of PAMAM dendrimers in the efficient transfer of genetic material into cells. Pharm Sci Technol Today 3:232–245

Fischer D, Li YX, Ahlemeyer B, Krieglstein J, Kissel T (2003) In vitro cytotoxicity testing of polycations: influence of polymer structure on cell viability and hemolysis. Biomaterials 24:1121–1131. doi:10.1016/S0142-9612(02)00445-3

Gimenez V, James C, Arminan A, Schweins R, Paul A, Vicent MJ (2012) Demonstrating the importance of polymer-conjugate conformation in solution on its therapeutic output: diethylstilbestrol (DES)-polyacetals as prostate cancer treatment. J Control Release 159:290–301. doi:10.1016/j.jconrel.2011.12.035

Haensler J, Szoka FC (1993) Polyamidoamine cascade polymers mediate efficient transfection of cells in culture. Bioconjugate Chem 4:372–379. doi:10.1021/Bc00023a012

Kaminskas LM et al (2014) Pulmonary administration of a doxorubicin-conjugated dendrimer enhances drug exposure to lung metastases and improves cancer therapy. J Control Release 183:18–26. doi:10.1016/j.jconrel.2014.03.012

Kono K, Akiyama H, Takahashi T, Takagishi T, Harada A (2005) Transfection activity of polyamidoamine dendrimers having hydrophobic amino acid residues in the periphery. Bioconjugate Chem 16:208–214. doi:10.1021/Bc049785e

Lopez-Montero I, Mateos-Gil P, Sferrazza M, Navajas PL, Rivas G, Velez M, Monroy F (2012) Active membrane viscoelasticity by the bacterial FtsZ-division protein. Langmuir 28:4744–4753. doi:10.1021/la204742b

Luque-Caballero G, Martin-Molina A, Sanchez-Trevino AY, Rodriguez-Valverde MA, Cabrerizo-Vilchez MA, Maldonado-Valderrama J (2014) Using AFM to probe the complexation of DNA with anionic lipids mediated by Ca2+: the role of surface pressure. Soft Matter 10:2805–2815. doi:10.1039/c3sm52428k

Ma Mintzer, Grinstaff MW (2011) Biomedical applications of dendrimers: a tutorial. Chem Soc Rev 40:173–190. doi:10.1039/b901839p

Maldonado-Valderrama J, Fainerman VB, Gálvez-Ruiz MJ, Martín-Rodriguez A, Cabrerizo-Vílchez MA, Miller R (2005) Dilatational rheology of β-casein adsorbed layers at liquid-fluid interfaces. J Phys Chem B 109:17608–17616. doi:10.1021/jp050927r

Maldonado-Valderrama J, Terriza JAH, Torcello-Gomez A, Cabrerizo-Vilchez MA (2013) In vitro digestion of interfacial protein structures. Soft Matter 9:1043–1053. doi:10.1039/c2sm26843d

Maldonado-Valderrama J, Torcello-Gomez A, Del Castillo-Santaella T, Holgado-Terriza JA, Cabrerizo-Vilchez MA (2014a) Subphase exchange experiments with the pendant drop technique. Adv Colloid Interface Sci. doi:10.1016/j.cis.2014.08.002

Maldonado-Valderrama J, Torcello-Gómez A, Castillo-Santaella TD, Holgado-Terriza JA, Cabrerizo-Vílchez MA (2014b) Subphase exchange experiments with the pendant drop technique Submitted

McCarthy JM, Appelhans D, Tatzelt J, Rogers MS (2013) Nanomedicine for prion disease treatment new insights into the role of dendrimers. Prion 7:198–202. doi:10.4161/Pri.24431

Merkel OM, Kissel T (2014) Quo vadis polyplex? J Control Release. doi:10.1016/j.jconrel.2014.06.009

Morales-Sanfrutos J, Megia-Fernandez A, Hernandez-Mateo F, Giron-Gonzalez MD, Salto-Gonzalez R, Santoyo-Gonzalez F (2011) Alkyl sulfonyl derivatized PAMAM-G2 dendrimers as nonviral gene delivery vectors with improved transfection efficiencies. Org Biomol Chem 9:851. doi:10.1039/c0ob00355g

Pavinatto FJ, Pavinatto A, Caseli L, Santos DS Jr, Nobre TM, Zaniquelli ME, Oliveira ON Jr (2007) Interaction of chitosan with cell membrane models at the air–water interface. Biomacromolecules 8:1633–1640. doi:10.1021/bm0701550

Peng JQ, Wu ZH, Qi XL, Chen Y, Li XB (2013) Dendrimers as potential therapeutic tools in HIV inhibition. Molecules 18:7912–7929. doi:10.3390/molecules18077912

Qamhieh K, Nylander T, Black CF, Attard GS, Dias RS, Ainalem M-L (2014) Complexes formed between DNA and poly(amido amine) dendrimers of different generations—modelling DNA wrapping and penetration. Phys Chem Chem Phys 16:13112–13122. doi:10.1039/c4cp01958j

Raykar PV, Fung MC, Anderson BD (1988) The role of protein and lipid domains in the uptake of solutes by human stratum-corneum. Pharm Res 5:140–150. doi:10.1023/A:1015956705293

Santos JL, Oliveira H, Pandita D, Rodrigues J, Pego AP, Granja PL, Tomas H (2010) Functionalization of poly(amidoamine) dendrimers with hydrophobic chains for improved gene delivery in mesenchymal stem cells. J Control Release 144:55–64. doi:10.1016/j.jconrel.2010.01.034

Shcharbin D, Pedziwiatr E, Bryszewska M (2009) How to study dendriplexes I: characterization. J Control Release 135:186–197. doi:10.1016/j.jconrel.2009.01.015

Shcharbin D, Pedziwiatr E, Blasiak J, Bryszewska M (2010) How to study dendriplexes II: transfection and cytotoxicity. J Controll Release 141:110–127. doi:10.1016/j.jconrel.2009.09.030

Shcharbin D, Shakhbazau A, Bryszewska M (2013) Poly(amidoamine) dendrimer complexes as a platform for gene delivery. Expert Opin Drug Del 10:1687–1698. doi:10.1517/17425247.2013.853661

Shcharbin D et al (2014) How to study dendrimers and dendriplexes III. Biodistribution, pharmacokinetics and toxicity in vivo. J Control Release 181:40–52. doi:10.1016/j.jconrel.2014.02.021

Somani S, Blatchford DR, Millington O, Stevenson ML, Dufes C (2014) Transferrin-bearing polypropylenimine dendrimer for targeted gene delivery to the brain. J Control Release 188C:78–86. doi:10.1016/j.jconrel.2014.06.006

Wege HA, Holgado-Terriza JA, Cabrerizo-Vilchez MA (2002) Development of a constant surface pressure penetration langmuir balance based on axisymmetric drop shape analysis. J Colloid Interface Sci 249:263–273. doi:10.1006/jcis.2002.8233

Yoo H, Juliano RL (2000) Enhanced delivery of antisense oligonucleotides with fluorophore-conjugated PAMAM dendrimers. Nucl Acids Res 28:4225–4231. doi:10.1093/nar/28.21.4225